IP3 receptors and Orai channels in pancreatic acinar cells: co-localisation and its consequences

György Lur, Mark W Sherwood, Etsuko Ebisui, Lee P Haynes, Stefan Feske, Robert Sutton, Robert Burgoyne, Katsuhiko Mikoshiba, Ole H Petersen, Alexei V Tepikin

IP_3 receptors and Orai channels in pancreatic acinar cells: co-localisation and its consequences

Gyorgy Lur[*], Mark W. Sherwood[†], Etsuko Ebisui†, Lee Haynes[*], Stefan Feske[‡], Robert Sutton[§], Robert D. Burgoyne[*], Katsuhiko Mikoshiba[†], Ole H. Petersen‖ and Alexei V. Tepikin[*].

[*]Department of Cellular and Molecular Physiology and [§]Liverpool NIHR Pancreas Biomedical Research Unit, The University of Liverpool, Crown Street, Liverpool L69 3BX, UK.

[†]Laboratory for Developmental Neurobiology, Riken Brain Science Institute, 2-1 Hirosawa, Wako City, Saitama, 351-0198 Japan.

[‡]NYU Langone Medical Centre, 550 First Avenue, SRB 316, New York, NY 10016, USA.

‖MRC Group, School of Biosciences, Cardiff University, Museum Avenue, Cardiff CF10 3AX, Wales, UK

Correspondence to:
Alexei V. Tepikin
Phone: +44 (0) 151 7945351
Fax: +44 (0) 151 7945327
E-mail: a.tepikin@liv.ac.uk

Short title: Orai1 co-localises with IP_3 receptors

Abbreviations: PAC, pancreatic acinar cells; ER, endoplasmic reticulum; SOCE, store-operated Ca^{2+} entry; STIM, stromal interaction molecule; IP_3R, IP_3 receptors; ACh, acetylcholine; CCK, cholecystokinin; $[Ca^{2+}]c$, cytosolic Ca^{2+} concentration; ZO1, zona occludens 1; TG thapsigargin.

Synopsis

Orai1 proteins have been recently identified as subunits of store-operated Ca^{2+} entry (SOCE) channels. In primary isolated pancreatic acinar cells, Orai1 showed remarkable co-localisation and co-immunoprecipitation with all 3 subtypes of IP_3 receptors. The co-localization between Orai1 and IP_3Rs was restricted to the apical part of pancreatic acinar cells. Neither co-localization nor co-immunoprecipitation was affected by the Ca^{2+} store depletion. Importantly we also characterised Orai1 in basal and lateral membranes of pancreatic acinar cells. The basal and lateral membranes of pancreatic acinar cells have been previously shown to accumulate STIM1 puncta as a result of store depletion. We therefore conclude that these polarized secretory cells contain two pools of Orai1 – apical that interact with IP_3Rs and baso-lateral that interact with STIM1 following the Ca^{2+} store depletion. Experiments on IP_3Rs knockout animals demonstrated that the apical Orai1 localization does not require IP_3Rs and that IP_3Rs are not necessary for the activation of SOCE. However, the IP_3-releasing secretagogue acetylcholine (ACh) produced a negative modulatory effect on SOCE, suggesting that activated IP_3Rs could have an inhibitory effect on this Ca^{2+} entry mechanism.

Keywords: Orai1; store-operated Ca^{2+} entry; IP_3 receptors; pancreatic acinar cells; acetylcholine; Ca^{2+} signalling.

Introduction

Pancreatic acinar cells (PAC) are structurally and functionally polarised with secretory granules located in the apical region, whilst the basal and lateral parts contain well-developed rough endoplasmic reticulum (ER). Thin projections of ER are also present in the apical region [1]. Important secretagogues such as acetylcholine (ACh) and cholecystokinin (CCK) utilise IP_3 and Ca^{2+} signalling cascades to regulate secretion in these cells [2]. The substantial Ca^{2+} extrusion by the plasma membrane Ca^{2+} ATPases (PMCAs) in PAC [3] necessitates a well-developed SOCE mechanism. IP_3R2 and IP_3R3 were shown to be the functional IP_3Rs in PAC [4]. Local apical Ca^{2+} transients can be triggered by IP_3 [5, 6]. All 3 types of IP_3Rs are found in the apical part of the cell [7-9]. The role of IP_3Rs in the activation of SOCE has been the subject of much debate [10]. The original conformational coupling hypothesis suggested that IP_3Rs in the store activate Ca^{2+} entry channels [11, 12]. It was later found that STIM proteins serve as the Ca^{2+} sensors in the store; the depletion of ER Ca^{2+} results in the translocation of STIM to the plasma membrane, where it interacts with and activates Orai channels [13-16]. The notion of conformational coupling was therefore confirmed, however with STIM rather than IP_3R as the primary ER Ca^{2+} sensor. This does not exclude that IP_3Rs could play some regulatory role in SOCE, particularly considering a recent report describing an interaction between IP_3Rs and Orai1 [17]. In PAC STIM1 was found to form puncta in the basal and lateral subplasmalemmal regions, where it was also shown to co-localise with Orai1 [18]. The basolateral SOCE in PAC is therefore mediated by STIM1 interacting with Orai1. Surprisingly, the highest density of Orai1 was found in the apical region – away from its activator STIM1 [18], but in the area populated with IP_3Rs [7-9]. This surprising finding led us to examine the relative positioning of the two proteins, which were found to be closely co-localised. In the second part of the study we probed the functional consequences of this co-localisation.

Materials and Methods.

Chemicals: All salts as well as Acetylcholine (ACh), goat serum, BSA and PBS were obtained from SIGMA (Gillingham, UK). Collagenase was from Worthington (Lorne Laboratories, Reading, UK). Thapsigargin and caffeine were from Calbiochem (San Diego, CA, USA). Protease inhibitor cocktail was from Roche Diagnostics (Mannheim, Germany). Protein G sepharose beads were from GE Healthcare (Uppsala, Sweden). Clean Blot reagent was from Pierce (Rockford, IL, USA). Fura-2 AM and Fluo-4 AM were from Invitrogen (Paisley, UK).

Animals and cell isolation. All animal experiments were conducted in accordance with the Animals (Scientific Procedure) Act of 1986. PAC were isolated from the pancreata of CD1 or BL6 (wild type or specified knockout) mice using collagenase digestion as described previously [3].

Immunofluorescence. Freshly isolated PAC were fixed in methanol for 10 minutes at -20°C. Nonspecific antibody binding was blocked for 1 hour in 10% goat serum and 1%

BSA prior to incubation with primary antibodies for 1 hour. IP_3 receptors were visualized by IP_3R3 antibodies (BD Transduction Laboratories, Franklin Lakes, NJ, USA) or IP_3R2 antibodies (rabbit polyclonal, raised against the C-terminal amino acids 2686-2702; a gift from Professor D. Yule, University of Rochester, USA) or IP_3R1 antibodies (rabbit polyclonal, raised against C-terminal amino acids 2735–2749 of mouse IP_3R1; a gift from Professor J. Parys from the University of Leuven). Orai1 channels were stained with an Orai1 antibody (rabbit polyclonal, raised against C terminal amino acids 278-294, produced by Dr. S. Feske) and tight junctions were visualized by occludin antibodies (Zymed Laboratories, Invitrogen, Carlsbad, CA, USA) or ZO1 antibodies (a gift from Dr. M. Furuse from Kobe University). Appropriate secondary antibodies conjugated to Alexa 488, Alexa 594 and/or Alexa 647 (Invitrogen, Paisley, UK) were applied for 30 minutes and cover slips were mounted on microscope slides with Prolong Gold (Invitrogen, Paisley, UK). All fluorescent secondary antibodies, used in the study, were tested on PAC fixed with the same method but without the application of a primary antibody. None of these secondary antibodies produced any nonspecific staining in PAC. Cells were viewed on a Leica TCS SP2 AOBS inverted confocal microscope (Leica Microsystems, Mannheim, Germany) equipped with a ×63 oil immersion objective (N.A. 1.4). Optical sections were spaced by 0.5-1µm. Linear adjustments of contrast and brightness were applied if necessary in Leica Application Suite.

Ca^{2+} imaging. Freshly isolated PAC were loaded with 2.5µM Fura-2 AM or 2.5µM Fluo-4 AM for 30 minutes at room temperature. Fluo-4 labelling was used for experiments involving caffeine. Standard Na-HEPES based extracellular solution contained (in mM): NaCl: 140; KCl: 4.7; Hepes: 10; $MgCl_2$: 1; glucose: 10; $CaCl_2$: 1; pH 7.4. In specific experiments the Ca^{2+} concentration in this solution was modified (i.e. reduced to nominally Ca^{2+} free or increased to 2mM). For Fura-2 imaging we utilised Till Photonics Imaging System (TILL Photonics GmbH, Germany) or a BSI Olympus Collaboration Centre Imaging System (RIKEN, Saitama, Japan). Fura-2 was excited at 340nm and 380nm, emission was collected using 510nm high pass filter. Experiments with Fluo-4 loaded cells were conducted on the Till Photonics imaging system. Fluo-4 labelling was used for experiments involving caffeine because of the strong effect of caffeine on the fluorescence of Fura-2. Fluo-4 was excited by at 470nm and emission was collected through a 510nm high pass filter.

Co-immunoprecipitation and Western blotting: PAC were lysed in IP buffer containing 50mM Tris, 150mM NaCl, 1% Triton X-100, 0.25% sodium-deoxy-cholate, 0.2% sodium-dodecil-sulphate, 2mM EDTA, 2x protease inhibitor cocktail. In each condition lysate containing 600µg protein was added to 2µg of IP_3 receptor antibody (described above) and mixed with 20µl protein G sepharose beads in a total volume of 1ml of IP buffer for 2 hours at 4°C. Proteins were eluted, separated on a 4-12% Tris-Glycine gradient gel and transferred onto nitrocellulose membranes (VWR). Following blocking in 5% milk for 1 hour, membranes were probed with Orai1 antibodies (Alomone Labs, Israel) and IP_3 receptor antibodies or actin antibodies (SIGMA, Gillingham, UK). Following staining with Clean Blot, bands were visualized using ECL western blotting substrate in a BioRad gel documentation system. Bands were quantified using ImageJ gel quantification plug-in.

Results

Orai1 co-localises with IP_3Rs in the apical pole of pancreatic acinar cells.

In the apical pole of PAC we found a striking co-localisation of endogenous Orai1 and IP_3R3 (Fig 1A, n=7). IP_3R2 and IP_3R3 are also co-localised in this cellular region (Fig 1B, n=6). The highest density of IP_3R1 was observed in the apical region where it co-localised with IP_3R3 (Fig 1C, n= 6). We can therefore conclude that Orai1 closely co-localises with all types of IP_3Rs in the apical pole of PAC. The apical localisation of Orai1 and its co-localisation with IP_3R3 did not change in conditions when the cells were treated with the IP_3-generating secretagogue ACh (S Fig 1A, n=3), the IP_3R inhibitor caffeine (S Fig 1B, n=3), or the SERCA pump inhibitor thapsigargin (S Fig 1C, n=3). Orai1 co-immunoprecipitated with all types of IP_3Rs (Fig 1D. n=6 for Orai1 and IP_3R1; n=7 for Orai1 and IP_3R2; n=16 for Orai1 and IP_3R3). This co-immunoprecipitation also did not change significantly when the cells were treated with ACh, (Fig 1D. n=6 for Orai1 and IP_3R1; n=7 for Orai1 and IP_3R2; n=14 for Orai1 and IP_3R3), caffeine (Fig 1D. n=3 for Orai1 and IP_3R1; n=5 for Orai1 and IP_3R2; n=4 for Orai1 and IP_3R3;), or thapsigargin (TG, Fig 1D. n=3 for Orai1 and IP_3R1; n=5 for Orai1 and IP_3R2; n=4 for Orai1 and IP_3R3). Importantly actin (which is present at high density in the apical region) was not co-immunoprecipitated with IP_3 receptors (S Fig 2, n=4). The observed co-immunopreciptation of Orai1 and IP_3Rs does not of course guarantee that there is a direct interaction between these proteins but it is unlikely that the co-immunoprecipitation is due to the interaction of the proteins with actin.

It is essential to note that unlike IP_3Rs, Orai1 was observed not only in the apical region, but also on the basal and lateral membranes (shown by arrows on Fig 1A). This was particularly evident in the optical sections that were recorded below (Fig 2A section at +5µm) or above (see Fig 2C section at +23µm) the apical region of the cells. Orai1 was clearly present outside the apical region, but the intensity of its immunostaining increased substantially in the apical region decorated with IP_3Rs (see Fig 2B section at +14µm) and in this region Orai1 was always found in the close vicinity of IP_3Rs (Fig 1, Fig 2B section at +14µm and S Fig 1).

Orai1 distribution in pancreatic acinar cells lacking IP_3 receptors.

To find out if the IP_3Rs are required for the apical positioning of Orai1, we imaged the distribution of Orai1 in PAC from IP_3R2 knockout (KO) mice, from $IP_3R2/3$ double KO mice [4] and from IP_3R1 KO mice [19] produced in K. Mikoshiba`s laboratory. The apical membrane region of PAC is enriched with occludin and zona occludens 1 (ZO1) (S Fig 3). As the apical pole cannot be visualized using IP_3R antibodies in the cells from the double KO animals, we used tight junction markers - occludin antibodies and/or ZO1 antibodies - to reveal the apical regions in clusters of acinar cells (both antibodies give very similar staining (S Fig 3) and were co-localised with IP_3Rs in the cells from the wild type animals (S Fig 4)). In the wild type animals Orai1 was mainly found co-localised with these proteins in the apical region, but was also present in the lateral and basal membranes (Fig 3A and S Movie 1). The distribution of Orai1 in PAC of KO animals was similar to that observed in cells from the wild type animals (Fig 3). Prominent apical

Orai1 staining was present in cells lacking IP_3R2 or both IP_3R2 and IP_3R3 or IP_3R1 (Fig 3B-D; n=5 for both IP_3R2 KO mice and for $IP_3R2/3$ double KO mice, n=3 for IP_3R1 KO mice). The basolateral presence of Orai1 was also unchanged in the cells from single and double IP_3Rs KO animals (Fig 3). These experiments suggest that IP_3Rs are not required for the targeting of Orai1 to basolateral or apical membrane regions of the PAC.

Effects of the IP_3-generating secretagogue ACh and the IP_3R inhibitor caffeine on SOCE in PAC from the wild type and IP_3Rs KO mice.

In these experiments thapsigargin (TG) was used to deplete Ca^{2+} stores in cells maintained in nominally Ca^{2+} - free extracellular solution. Addition of Ca^{2+} to the extracellular solution resulted in SOCE-mediated increase in cytosolic Ca^{2+} ($[Ca^{2+}]c$) followed by formation of an elevated $[Ca^{2+}]c$ plateau (Fig 4). Addition of IP_3 – producing secretagogue ACh reversibly decreased the amplitude of the plateau (Fig 4A, n=465). Using the Mn quench technique [20] we also observed a small (13 ± 2 %) but statistically significant inhibition of the influx by 300nM ACh (S Fig 5, n=145 cells in ACh - treated group and n=139 cells in control group). Caffeine (10mM), which in PAC very efficiently blocks IP_3 – induced Ca^{2+} responses [21] has no effect on its own (Fig 4B, n= 169), but it partially reversed the ACh–induced reduction of the plateau (Fig 4C, n=168). These experiments suggest that activation of IP_3Rs has a mild inhibitory rather than stimulatory action on SOCE. Caffeine efficiently quenches fura-2, because of this property the experiments described above were conducted using single wavelength indicator fluo-4. We further tested the effects of ACh on TG-induced $[Ca^{2+}]c$ plateau using the ratiometric probe fura-2. The results were similar to that observed using fluo-4 i.e. 300nM ACh (but not 50nM ACh) reversibly decreased TG-induced $[Ca^{2+}]c$ plateau (Fig 5A and B, n= 61 for 50nM ACh and n=62 for 300nM ACh). Similar results were found in experiments on PAC from IP_3R2 KO mice (Fig 5C and D, n=47 for 50nM ACh and n= 33 for 300nM ACh) and from $IP_3R2/3$ double KO mice (Fig 5E and F, n= 46 for 50nM ACh and n= 31 for 300nM ACh) although the recovery phase (on removal of ACh) was less clear in experiments on KO and double KO mice. To assess SOCE more directly and provide an internal control for each experiment we used a two pulse protocol, where cellular Ca^{2+} stores were depleted using TG in nominally Ca^{2+}-free external solution and then two short pulses of extracellular calcium (2mM) were applied (Fig 6A). The first pulse (after the TG-induced Ca^{2+} store depletion) was applied in agonist-free extracellular medium, whilst the second pulse was applied in the presence of ACh (Fig 6A) or in agonist-free extracellular medium (control, not shown). The changes in the Fura-2 340nm/380nm ratio were differentiated (the procedure is illustrated on the insert in Fig 6A) and the maximal rate determined. Considering the relatively slow Ca^{2+} extrusion by PMCA at or near the resting $[Ca^{2+}]c$ [3] and taking into account that the maximal rates of changes were also observed at close to resting $[Ca^{2+}]c$, we can assume that the maximal derivative reflects the maximal SOCE rate. The maximal SOCE rate during the second pulse was normalized to that recorded during the first pulse, in order to provide an internal control for every cell in each experiment (Fig 6A and B). In wild type cells, a low concentration of ACh (50nM) slightly reduced the SOCE rate (by 10±3%, n=61; Fig 6B), whilst the treatment with 300nM ACh resulted in a reduction in the SOCE rate of 27±4% (n=62, Fig 6B). In similar experiments (S Fig 6) we tested the effect of caffeine on SOCE rate. Caffeine (10mM) alone did not affect SOCE rate (S Fig 6, n=48).

The ability of ACh to inhibit SOCE was further tested using the two pulse protocol on the PAC from IP_3R2 single KO and $IP_3R2/3$ double KO mice (Fig 6C-F). These experiments showed that both concentrations of ACh induced small, but statistically significant, reductions in the SOCE rate in PAC from IP_3R2 KO mice (Fig 6C and 6D). Both concentrations reduced SOCE rate by 20±2%. These results were qualitatively similar to those obtained in cells from wild type animals. The Ca^{2+} responses in cells from the $IP_3R2/3$ double KO mice were different - the response to TG was drastically reduced in comparison with that in the wild type and the single KO mice (Fig 6E compare with 6A and 6C). This suggests that IP_3Rs amplify TG response by Ca^{2+}-induced Ca^{2+} release and that this amplification mechanism is absent in $IP_3R2/3$ double KO mice. The responses to the external Ca^{2+} pulses in PAC from the double KO mice were, however, surprisingly robust (Fig 6E). In fact the maximal SOCE rate during the first pulse was slightly higher in the cells from the double KO mice (26% higher) than the single KO mice. Using the two pulse protocol we have not observed changes in the SOCE rate upon application of 50nM or 300nM ACh in the cells from double KO animals (Fig 6F, n=67 for 50nM and n=76 for 300nM). The SOCE rate during the second pulse was however already reduced by approximately 20% in comparison with the first pulse even in control (no ACh) conditions (Fig 6F). It is therefore possible that we do not observe ACh-induced SOCE suppression in these experiments because the ACh simply cannot inhibit the Ca^{2+} influx any further.

Discussion

PAC structurally satisfy the requirements for IP_3R and SOC channel interaction (see Fig 1) suggested as the basis for the original conformational-coupling theory of SOCE [11, 12]. We were not able to detect SOCE up-regulation in response to stimulation with the IP_3-producing agonist ACh. The inhibition of IP_3Rs with caffeine also had no affect on SOCE. In these respects the study yielded important negative results. This finding is in line with conclusions from the study by Woodard and colleagues [17], which highlighted the importance of the interaction between IP_3Rs and Orai1 for different Ca^{2+} signalling processes, but indicated that the disruption of the interaction between IP_3R1 and Orai1 does not prevent TG-induced SOCE and has no significant effect on this process.

The ACh application experiments suggest that IP_3Rs could negatively regulate SOCE. This negative modulation could offer some protection against Ca^{2+} overload induced by IP_3 - producing secretagogues. The effect of ACh is however moderate and SOCE develops efficiently in the acinar cells lacking both functional types of IP_3Rs.

In our study the highest density of Orai1 was observed in the apical part of the cell containing IP_3Rs, occludin and ZO-1. Importantly, we also found Orai1 along the lateral and basal membranes - far beyond the region containing tight junctions and IP_3Rs (Fig 1, 2, 3 and Movie S1). In this basolateral region, Orai1 was shown to co-localise with STIM1 and form Orai1 and STIM1 puncta following ER store depletion [18]. It is possible that two mechanisms of SOCE operate in PAC; baso-lateral SOCE mediated by STIM1 and Orai1 proteins will have a reliable Ca^{2+} source delivered by the interstitial fluid, whilst apical SOCE could help to re-capture Ca^{2+} transported paracellularly [22], extruded by PMCA (which are active in the apical region [23, 24]) and exocytosed with the content of secretory granules. It is conceivable that apical Orai1 could play a role in

preventing the build-up of Ca^{2+} in pancreatic ducts, and consequently, pancreatic stone formation in these structures. The close co-positioning of IP_3Rs and Orai1 in the apical region suggests that if activated the apical Orai1 could efficiently re-load strategically important (IP_3R containing) Ca^{2+} stores. The ability of the apical Orai1 to participate in SOCE, the putative mechanism of activation and the physiological function of the apical Orai1 will need to be determined in a separate study. While this paper was in revision a study was published by J. Hong and colleagues [25] indicating that Orai1 is localised in the apical part of acinar cells were it co-localised with IP_3R3. The important difference between this study and our paper is that we observed a substantial presence of Orai1 in the plasma membrane regions outside the apical pole. Indeed our confocal images (Fig 1, S Fig 1, Fig 3, S Movie 1 and particularly Fig 2) clearly reveal substantial Orai1 staining outside the plasma membrane regions decorated with IP_3Rs, occludin or ZO-1. Also contrary to conclusions from Hong's study (but see Fig 5A from Hong's paper), in our previous work we have not observed apical localisation of STIM1 in cells with depleted ER Ca^{2+} stores [18]. We therefore consider that the apical function of Orai1 is likely to be STIM1- independent. It is also important to note that the previous electron microscopy investigation of the sub-plasmalemmal ER and the plasma membrane in pancreatic acinar cells, revealed ribosome-free rough ER junctions decorated with STIM1 in basal and lateral sub-plasmalemmal regions, but not in the apical pole of the cell [18]. It is therefore difficult to reconcile some of the conclusions (specifically the role of STIM1 in activating apical Orai1 channels) of Hong's paper and our study.

The current work revealed close positioning of IP_3Rs and Orai1 channels in the apical pole of the PAC , documented the presence of Orai1 in the apical region of the cells lacking functional IP_3Rs and concluded that, in spite of the remarkably close localisation of the two proteins, IP_3Rs do not activate SOCE in the apical region of PAC.

Figure Legends.

Figure 1. Orai1 co-localisation and co-immunoprecipitation with IP_3 receptors in pancreatic acinar cells.
(A) Maximum projection of 20 optical sections spaced 1μm from each other in a PAC cluster. Orai1 (green) is present in both the basolateral (arrows) and apical (arrowheads) regions. In the apical pole Orai1 co-localises with IP_3R3 (magenta). Inserts show a single confocal section from the same cluster in higher magnification (the arrow and arrowhead points to the same structures as in the main figure). Here and on (B) and (C) the scale bars correspond to 10μm in the projections and 5μm in the inserts. **(B)** Maximum projection of optical sections of a PAC cluster. IP_3R2 (cyan) co-localises with IP_3R3 (magenta) in the apical pole of the cells (arrowhead). Inserts display a single confocal section from the same cluster in higher magnification (the arrowhead points to the same structures as in the main figure). **(C)** Maximum projection of optical sections of a PAC cluster. The highest density of IP_3R1 (yellow) is observed in the apical pole of the cells (arrowheads) where it co-localises with IP_3R3 (magenta). Inserts display a single confocal section from the same cluster in higher magnification (the arrowhead points to the same structures as in the main figure). Note that a significant staining for IP_3R1(unlike that for IP_3R2 and IP_3R3) was also found outside the apical region of the cell. (**D**) Co-immunoprecipitation of Orai1 with IP_3R1 (left panel), IP_3R2 (middle panel)

or with IP_3R3 (right panel) in PAC lysates. The first lane in both panels corresponds to beads that were not bound to anti-IP_3R antibodies. Western blots show the IP_3Rs and Orai1 eluted from sepharose beads decorated with the corresponding IP3Rs. Bar graphs show the quantification of Western blots.

Figure 2. Orai1 only co-localises with IP_3 receptors in the apical region of the acinar cells: apical and basolateral Orai1.

(A) Confocal section from a cluster of PAC recorded 5µm from the cover slip. This section is below the apical regions of the cells and Orai1 (green) is clearly visible in the basal and lateral membranes (arrows). **(B)** Confocal section from the same cluster as in (A) but recorded 14µm from the top of the cover slip where IP_3R3s (magenta) decorate the apical surfaces of the cells. Apical Orai1 present in this section (arrowhead) co-localises with the IP_3R3s. **(C)** Confocal section of the same acinar cell cluster as in (A) and (B). Confocal section was positioned 23µm from the cover slip. IP_3Rs are no longer visible as this section is above the apical regions of the cells; however Orai1 is still present in the lateral and basal membranes (arrows). Scale bars correspond to 5µm.

Figure 3. Orai1 is present in the apical pole of acinar cells lacking IP_3 receptors.

(A) Confocal section of an acinar cell cluster isolated from wild type mouse. Orai1 (green) is visible in basolateral membranes (arrows) and in the apical pole (arrowheads) where it co-localises with tight junctions (red) marking the apical membrane. **(B)** Confocal section of a cluster of acinar cells isolated from IP_3R2 KO mice. Orai1 is apparent in both apical (arrowhead) and basolateral membranes (arrows), its distribution is similar to that in the cells from wild type animals. **(C)** Confocal section of an acinar cell cluster isolated from mice lacking both IP_3R2 and IP_3R3 ($IP_3R2/3$ KO). Orai1 is present in basolateral membranes (arrow) as well as in the apical pole (arrowhead) where it co-localises with tight junction markers. (**D**) Confocal section of an acinar cell cluster isolated from IP_3R1 KO mice. Orai1 staining is visible in the apical pole (arrowhead) and in basolateral membranes (arrow). Scale bars represent 5µm.

Figure 4. Effect of ACh and caffeine on the cytosolic Ca^{2+} plateau in pancreatic acinar cells.

(A) TG (2µM) induced depletion of the ER Ca^{2+} stores in cells placed in the nominally Ca^{2+} free extracellular solution. Subsequent addition of 2mM Ca^{2+} to the extracellular solution resulted in the increase of $[Ca^{2+}]c$. ACh application (following the formation of the plateau) caused a decrease in the level of cytosolic Ca^{2+}. Removal of ACh resulted in partial restoration of the amplitude of $[Ca^{2+}]c$. (**B**) Application of caffeine (10mM) did not affect the $[Ca^{2+}]c$ plateau. Bar graph (see insert) shows the quantification of the amplitude of the $[Ca^{2+}]c$ plateau before and after addition of caffeine. **(C)** Caffeine treatment partially reverses the effect of ACh on $[Ca^{2+}]c$ plateau. (**D**) Bar graph shows the quantification of the results illustrated on panels A-C. The amplitude of the $[Ca^{2+}]c$ plateau was measured before treatment (white bar), following the addition of ACh (striped bar), following the removal of ACh from the extracellular solution (cross-hatched

bar) or following the perfusion with the extracellular solution containing both ACh and caffeine (black bar). Symbol * indicates statistical significance ($p<0.05$).

Figure 5. Effect of ACh on the cytosolic Ca^{2+} plateau in acinar cells isolated from wild type and IP_3R KO mice.

(**A**) Intracellular Ca^{2+} stores of Fura-2 - loaded PAC, isolated from wild type mice, were depleted during a 30 min preincubation in nominally Ca^{2+} free extracellular solution containing 2μM thapsigargin (TG). The addition of 2mM Ca^{2+} to the extracellular solution resulted in the formation of a $[Ca^{2+}]c$ plateau. Subsequent ACh application triggered a small drop of the plateau that could be reversed by removal of ACh. (**B**) Bar graph shows the normalised (to the plateau level before ACh addition) plateau amplitude before (white bars) and following (striped bars) treatment with 50nM or 300nM ACh. Only the application of a large concentration of ACh (300nM) caused a significant reduction of the plateau amplitude in PAC from wild type mice (paired T-test, * indicates that $p<0.05$). (**C**) Intracellular Ca^{2+} stores of Fura-2 loaded PAC, isolated from IP_3R2 KO mice, were depleted with 2μM TG in nominally Ca^{2+} free extracellular solution and subsequent addition of 2mM Ca^{2+} resulted in the formation of a $[Ca^{2+}]c$ plateau. Application of a large concentration of ACh resulted in a small decrease of the plateau. (**D**) Bar graph shows the normalised plateau amplitude, recorded from PAC from IP_3R2 KO mice, before (white bars) and following (striped bars) treatment with 50nM or 300nM ACh. Only the application of a 300nM ACh caused a significant reduction of plateau amplitude in PAC from IP_3R2 KO mice (paired T-test, * indicates that $p<0.05$). (**E**) Intracellular Ca^{2+} stores of Fura-2 loaded PAC, isolated from $IP_3R2/3$ KO mice, were depleted as described above and cytosolic Ca^{2+} plateau was formed by introducing 2mM Ca^{2+} to the extracellular solution. Subsequent addition of ACh resulted in a decrease of cytosolic Ca^{2+} level. (**F**) Bar graph shows the normalised plateau amplitude, recorded from PAC from $IP_3R2/3$ KO mice before (white bars) and following (striped bars) treatment with 50nM or 300nM ACh. Only the application of a 300nM ACh caused a small but statistically significant reduction of plateau amplitude (paired T-test, * indicates that $p<0.05$).

Figure 6. Effects of ACh on the rate of SOCE in pancreatic acinar cells isolated from wild type and IP_3R KO mice. (**A**) Fura-2 ratio changes upon TG treatment and pulses of external Ca^{2+} in the absence and presence of 300nM ACh in PAC from the wild type animals. To assess the rate of Ca^{2+} influx the rising phase (induced by a short pulse of 2mM Ca^{2+}) of the curve was differentiated and the maximum rate of influx was estimated as the maximal value of the derivative (see insert). The same procedure was repeated for the second pulse of external Ca^{2+} (delivered in the presence or absence of ACh). **(B)** Summary of the effects of 50nM ACh and 300nM ACh on SOCE rate in the cells from wild type animals. Here, as well as in (D) and (F), the statistical significance was probed by ANOVA test; symbol * indicates $p<0.05$. (**C**) Fura-2 ratio changes upon TG treatment and pulses of external Ca^{2+} in the absence and presence of 300nM ACh in PAC from IP_3R2 KO mice. **(D)** Summary of the effects of 50nM and 300nM ACh on SOCE rate in the cells from IP_3R2 KO mice. **(E)** Fura-2 ratio changes upon TG treatment and pulses of external Ca^{2+} in the absence and presence of 300nM ACh in PAC from

$IP_3R2/3$ double KO mice. **(F)** Summary graph showing SOCE rate in control conditions and in the presence of 50nM or 300nM ACh in the cells from $IP_3R2/3$ double KO mice.

Acknowledgements

The support from RIKEN BSI-Olympus Collaboration Centre is gratefully acknowledged. Authors declare no conflict of interest, except S.F. who is a scientific co-founder of CalciMedica.

Funding

The work was supported by Medical Research Council (UK) grants G0700167 and G19/22, Wellcome Trust grant 080906/Z/06/Z, National Institute for Health Research (UK) grant to the Liverpool NIHR Pancreas Biomedical Research Unit. K. M. was supported by Japan Science and Technology Agency (Japan) grant (Ca^{2+} oscillations project). S. F. was supported by National Institute of Health (US) grant AI066128. M.S. is a RIKEN Foreign Postdoctoral Research Fellow.

REFERENCES

1. Park, M.K., Petersen, O.H., Tepikin, A.V. (2000) The endoplasmic reticulum as one continuous Ca(2+) pool: visualization of rapid Ca(2+) movements and equilibration. EMBO J. **19**, 5729-5739

2. Petersen, O.H., Tepikin, A.V. (2008) Polarized calcium signaling in exocrine gland cells. Annu.Rev.Physiol. **70**, 273-299

3. Tepikin, A.V., Voronina, S.G., Gallacher, D.V., Petersen, O.H. (1992) Pulsatile Ca2+ extrusion from single pancreatic acinar cells during receptor-activated cytosolic Ca2+ spiking. J.Biol.Chem. **267**, 14073-14076

4. Futatsugi, A., Nakamura, T., Yamada, M.K., Ebisui, E., Nakamura, K., Uchida, K., Kitaguchi, T., Takahashi-Iwanaga, H., Noda, T., Aruga, J., Mikoshiba, K. (2005) IP3 receptor types 2 and 3 mediate exocrine secretion underlying energy metabolism. Science. **309**, 2232-2234

5. Ito, K., Miyashita, Y., Kasai, H. (1997) Micromolar and submicromolar Ca2+ spikes regulating distinct cellular functions in pancreatic acinar cells. EMBO J. **16**, 242-251

6. Thorn, P., Lawrie, A.M., Smith, P.M., Gallacher, D.V., Petersen, O.H. (1993) Local and global cytosolic Ca2+ oscillations in exocrine cells evoked by agonists and inositol trisphosphate. Cell. **74**, 661-668

7. Lee, M.G., Xu, X., Zeng, W., Diaz, J., Wojcikiewicz, R.J., Kuo, T.H., Wuytack, F., Racymaekers, L., Muallem, S. (1997) Polarized expression of Ca2+ channels in

pancreatic and salivary gland cells. Correlation with initiation and propagation of [Ca2+]i waves. J.Biol.Chem. **272**, 15765-15770

8. Nathanson, M.H., Fallon, M.B., Padfield, P.J., Maranto, A.R. (1994) Localization of the type 3 inositol 1,4,5-trisphosphate receptor in the Ca2+ wave trigger zone of pancreatic acinar cells. J.Biol.Chem. **269**, 4693-4696

9. Yule, D.I., Ernst, S.A., Ohnishi, H., Wojcikiewicz, R.J. (1997) Evidence that zymogen granules are not a physiologically relevant calcium pool. Defining the distribution of inositol 1,4,5-trisphosphate receptors in pancreatic acinar cells. J.Biol.Chem. **272**, 9093-9098

10. Parekh, A.B., Putney, J.W., Jr. (2005) Store-operated calcium channels. Physiol Rev. **85**, 757-810

11. Berridge, M.J. (1995) Capacitative calcium entry. Biochem.J. **312 (Pt 1)**, 1-11

12. Irvine, R.F. (1990) 'Quantal' Ca2+ release and the control of Ca2+ entry by inositol phosphates--a possible mechanism. FEBS Lett. **263**, 5-9

13. Feske, S., Gwack, Y., Prakriya, M., Srikanth, S., Puppel, S.H., Tanasa, B., Hogan, P.G., Lewis, R.S., Daly, M., Rao, A. (2006) A mutation in Orai1 causes immune deficiency by abrogating CRAC channel function. Nature. **441**, 179-185

14. Liou, J., Kim, M.L., Heo, W.D., Jones, J.T., Myers, J.W., Ferrell, J.E., Jr., Meyer, T. (2005) STIM is a Ca2+ sensor essential for Ca2+-store-depletion-triggered Ca2+ influx. Curr.Biol. **15**, 1235-1241

15. Luik, R.M., Wu, M.M., Buchanan, J., Lewis, R.S. (2006) The elementary unit of store-operated Ca2+ entry: local activation of CRAC channels by STIM1 at ER-plasma membrane junctions. J.Cell Biol. **174**, 815-825

16. Roos, J., DiGregorio, P.J., Yeromin, A.V., Ohlsen, K., Lioudyno, M., Zhang, S., Safrina, O., Kozak, J.A., Wagner, S.L., Cahalan, M.D., Velicelebi, G., Stauderman, K.A. (2005) STIM1, an essential and conserved component of store-operated Ca2+ channel function. J.Cell Biol. **169**, 435-445

17. Woodard, G.E., Lopez, J.J., Jardin, I., Salido, G.M., Rosado, J.A. (2010) TRPC3 regulates agonist-stimulated Ca2+ mobilization by mediating the interaction between type I inositol 1,4,5-trisphosphate receptor, RACK1, and Orai1. J.Biol.Chem. **285**, 8045-8053

18. Lur, G., Haynes, L.P., Prior, I.A., Gerasimenko, O.V., Feske, S., Petersen, O.H., Burgoyne, R.D., Tepikin, A.V. (2009) Ribosome-free terminals of rough ER allow formation of STIM1 puncta and segregation of STIM1 from IP(3) receptors. Curr.Biol. **19**, 1648-1653

19. Matsumoto, M., Nakagawa, T., Inoue, T., Nagata, E., Tanaka, K., Takano, H., Minowa, O., Kuno, J., Sakakibara, S., Yamada, M., Yoneshima, H., Miyawaki, A., Fukuuchi, Y., Furuichi, T., Okano, H., Mikoshiba, K., Noda, T. (1996) Ataxia and epileptic seizures in mice lacking type 1 inositol 1,4,5-trisphosphate receptor. Nature. **379**, 168-171

20. Barrow, S.L., Voronina, S.G., da, S., X, Chvanov, M.A., Longbottom, R.E., Gerasimenko, O.V., Petersen, O.H., Rutter, G.A., Tepikin, A.V. (2008) ATP depletion inhibits Ca2+ release, influx and extrusion in pancreatic acinar cells but not pathological Ca2+ responses induced by bile. Pflugers Arch. **455**, 1025-1039

21. Toescu, E.C., O'Neill, S.C., Petersen, O.H., Eisner, D.A. (1992) Caffeine inhibits the agonist-evoked cytosolic Ca2+ signal in mouse pancreatic acinar cells by blocking inositol trisphosphate production. J.Biol.Chem. **267**, 23467-23470

22. Jansen, J.W., Schreurs, V.V., Swarts, H.G., Fleuren-Jakobs, A.M., de Pont, J.J., Bonting, S.L. (1980) Role of calcium in exocrine pancreatic secreation. VI. Characteristics of the paracellular pathway for divalent cations. Biochim.Biophys.Acta. **599**, 315-323

23. Belan, P.V., Gerasimenko, O.V., Tepikin, A.V., Petersen, O.H. (1996) Localization of Ca2+ extrusion sites in pancreatic acinar cells. J.Biol.Chem. **271**, 7615-7619

24. Lee, M.G., Xu, X., Zeng, W., Diaz, J., Kuo, T.H., Wuytack, F., Racymaekers, L., Muallem, S. (1997) Polarized expression of Ca2+ pumps in pancreatic and salivary gland cells. Role in initiation and propagation of [Ca2+]i waves. J.Biol.Chem. **272**, 15771-15776

25. Hong, J.H., Li, Q., Kim, M.S., Shin, D.M., Feske, S., Birnbaumer, L., Cheng, K.T., Ambudkar, I.S., Muallem, S. (2011) Polarized but Differential Localization and Recruitment of STIM1, Orai1 and TRPC Channels in Secretory Cells. Traffic. **12**, 232-245

Biochemical Journal Immediate Publication. Published on 03 Mar 2011 as manuscript BJ20110083

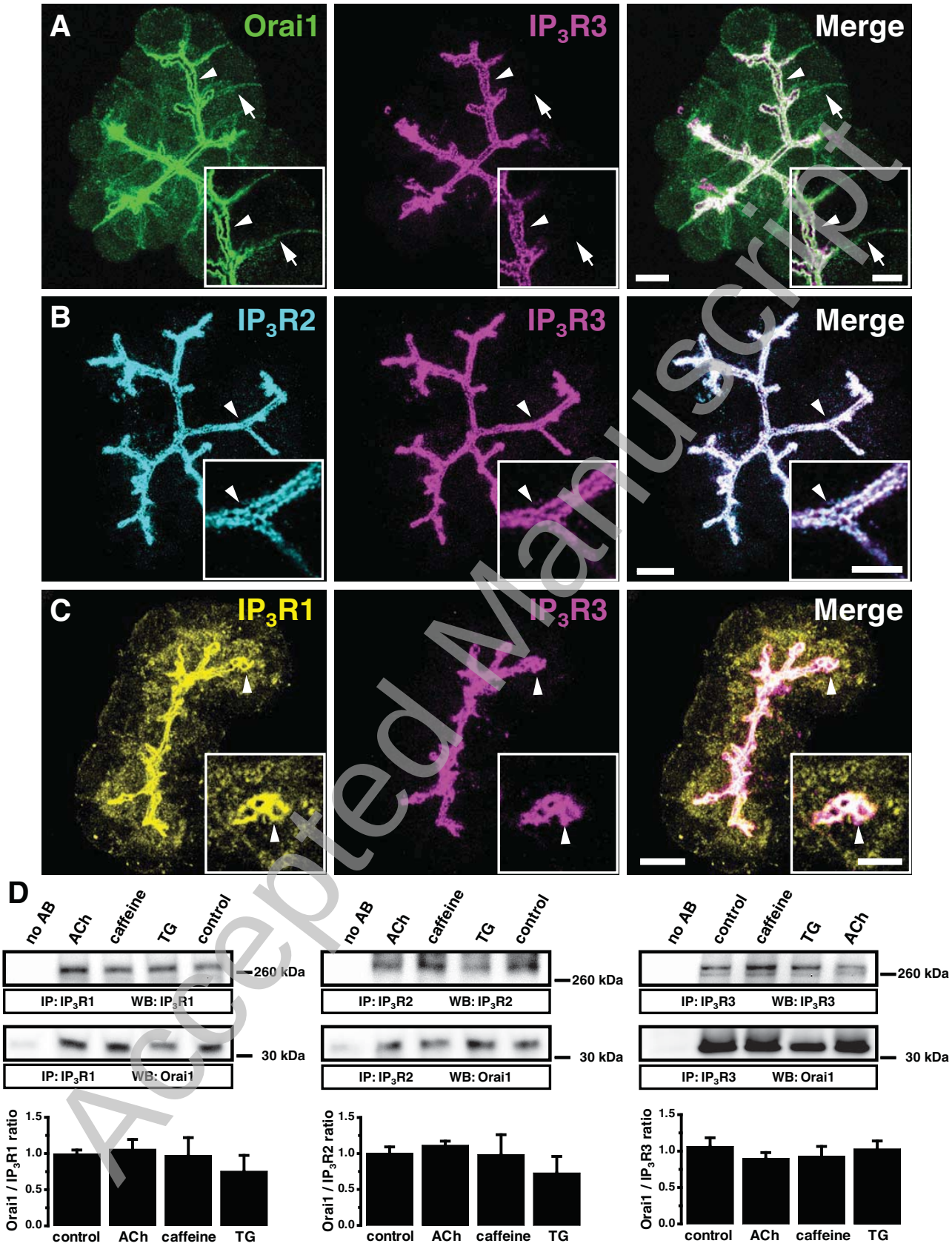

Figure 1

Biochemical Journal Immediate Publication. Published on 03 Mar 2011 as manuscript BJ20110083

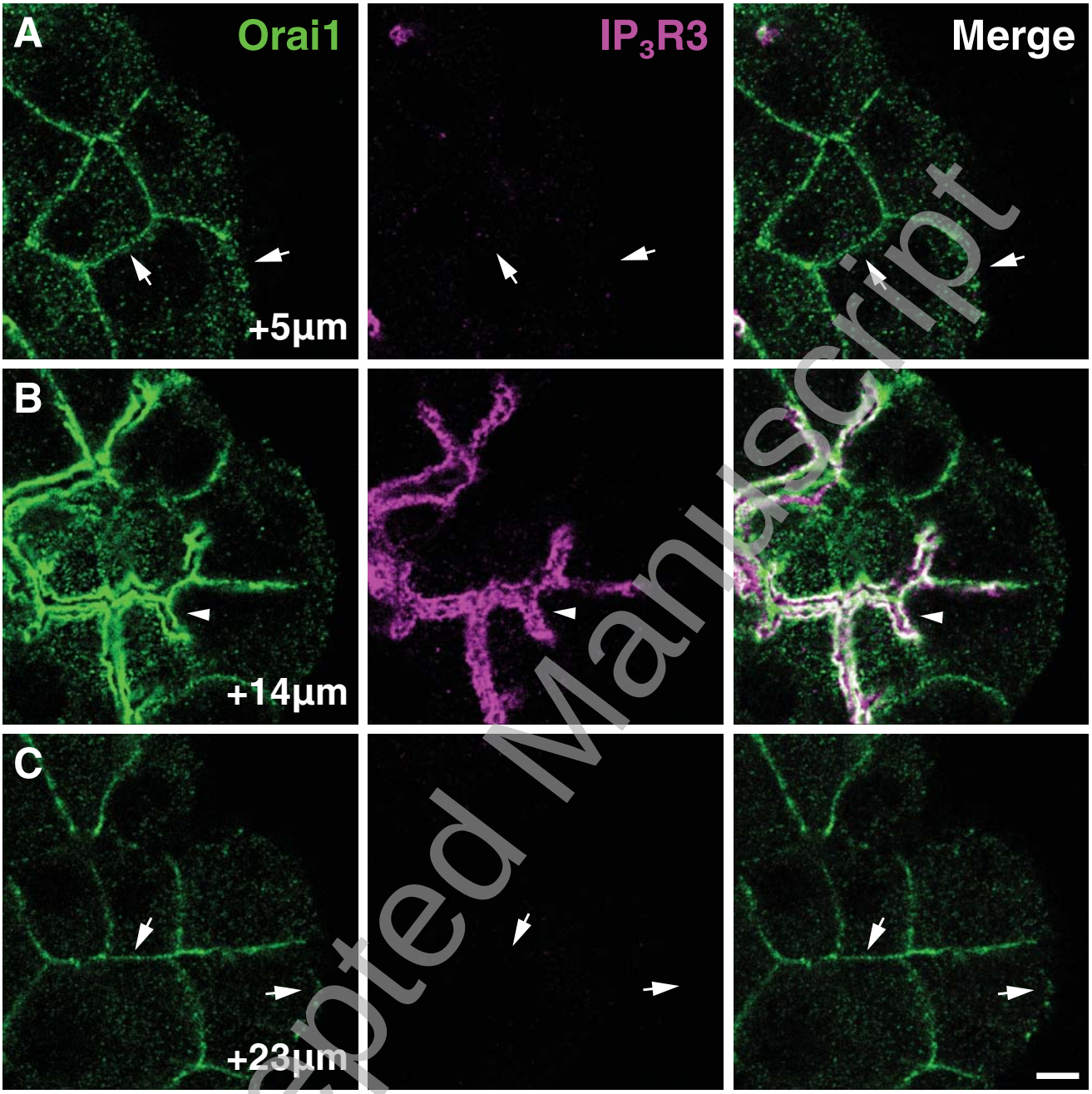

Figure 2

Biochemical Journal Immediate Publication. Published on 03 Mar 2011 as manuscript BJ20110083

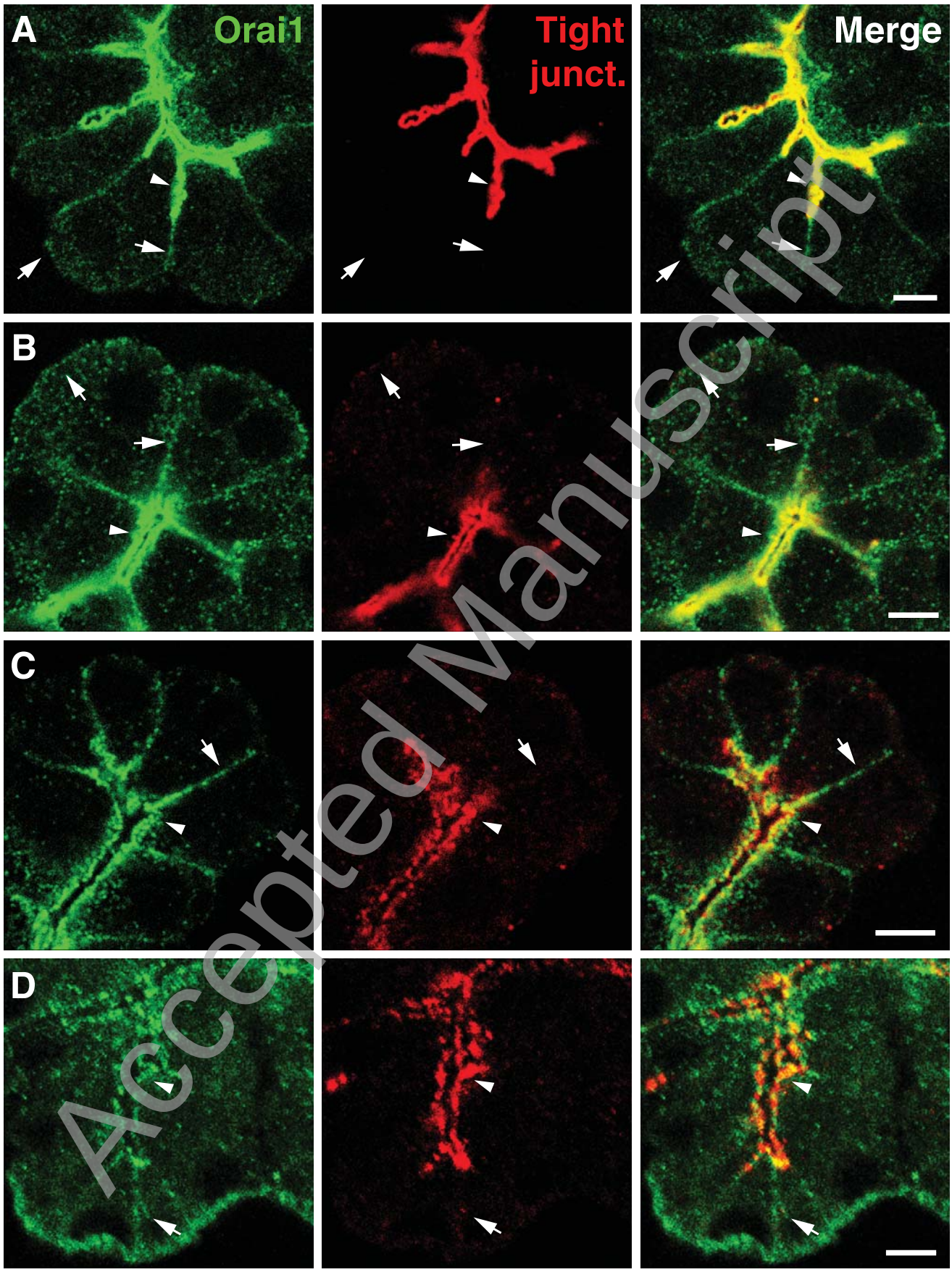

Figure 3

Biochemical Journal Immediate Publication. Published on 03 Mar 2011 as manuscript BJ20110083

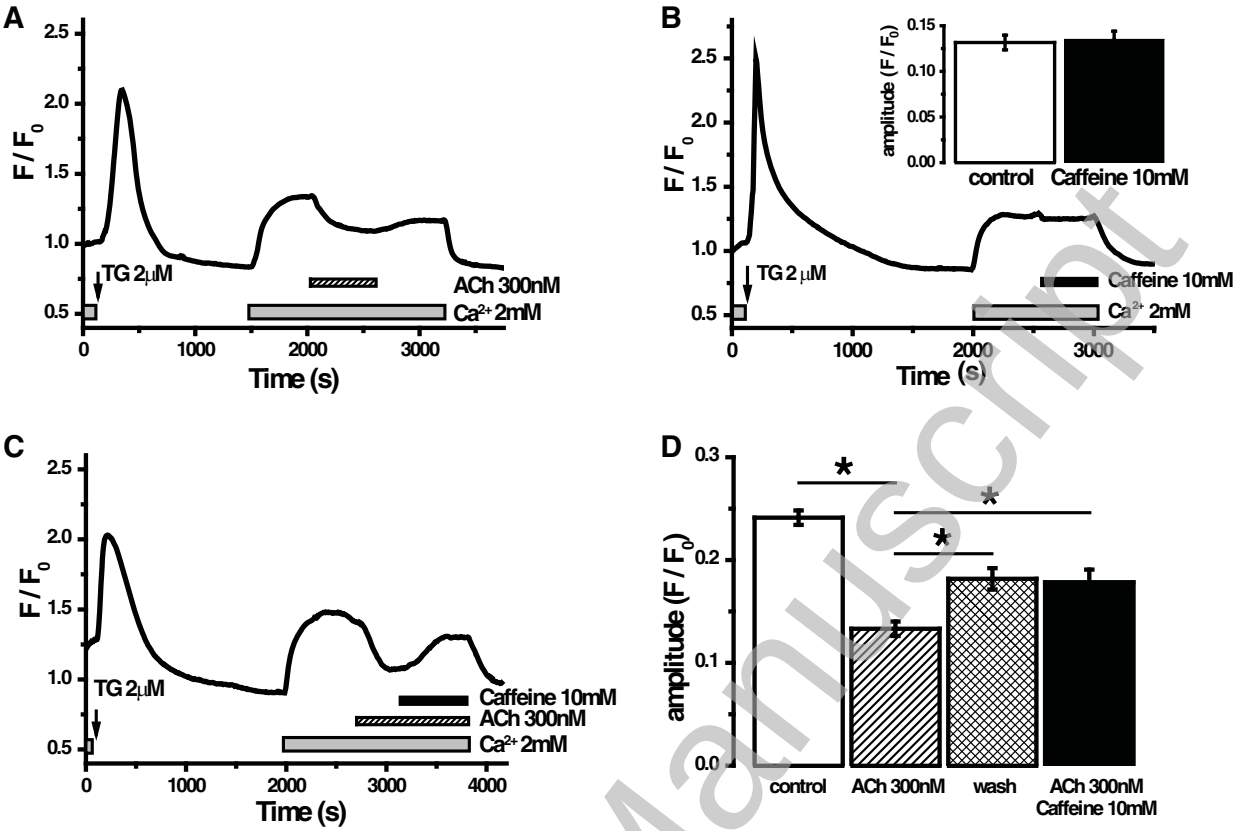

Figure 4

Biochemical Journal Immediate Publication. Published on 03 Mar 2011 as manuscript BJ20110083

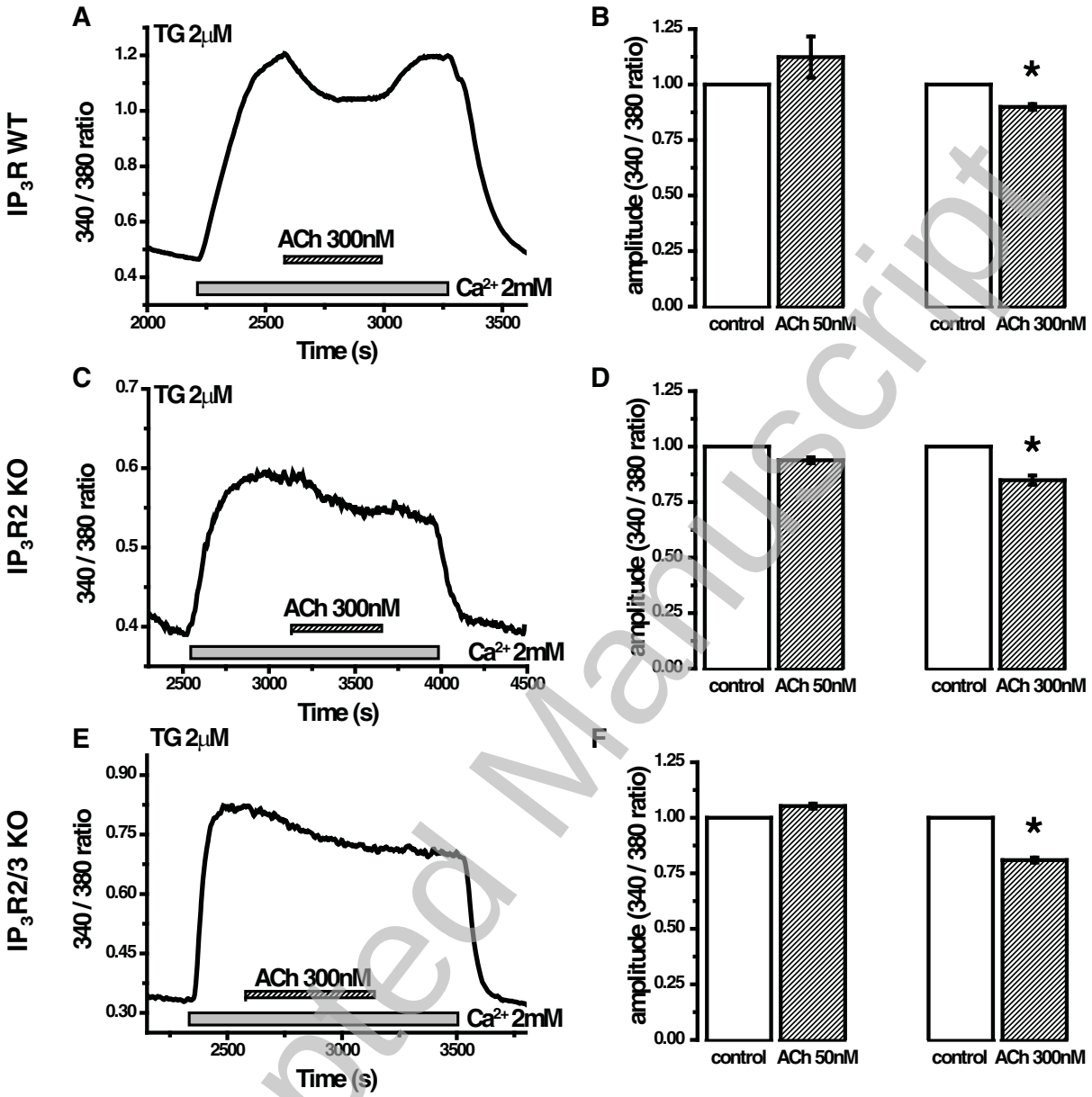

Figure 5

Biochemical Journal Immediate Publication. Published on 03 Mar 2011 as manuscript BJ20110083

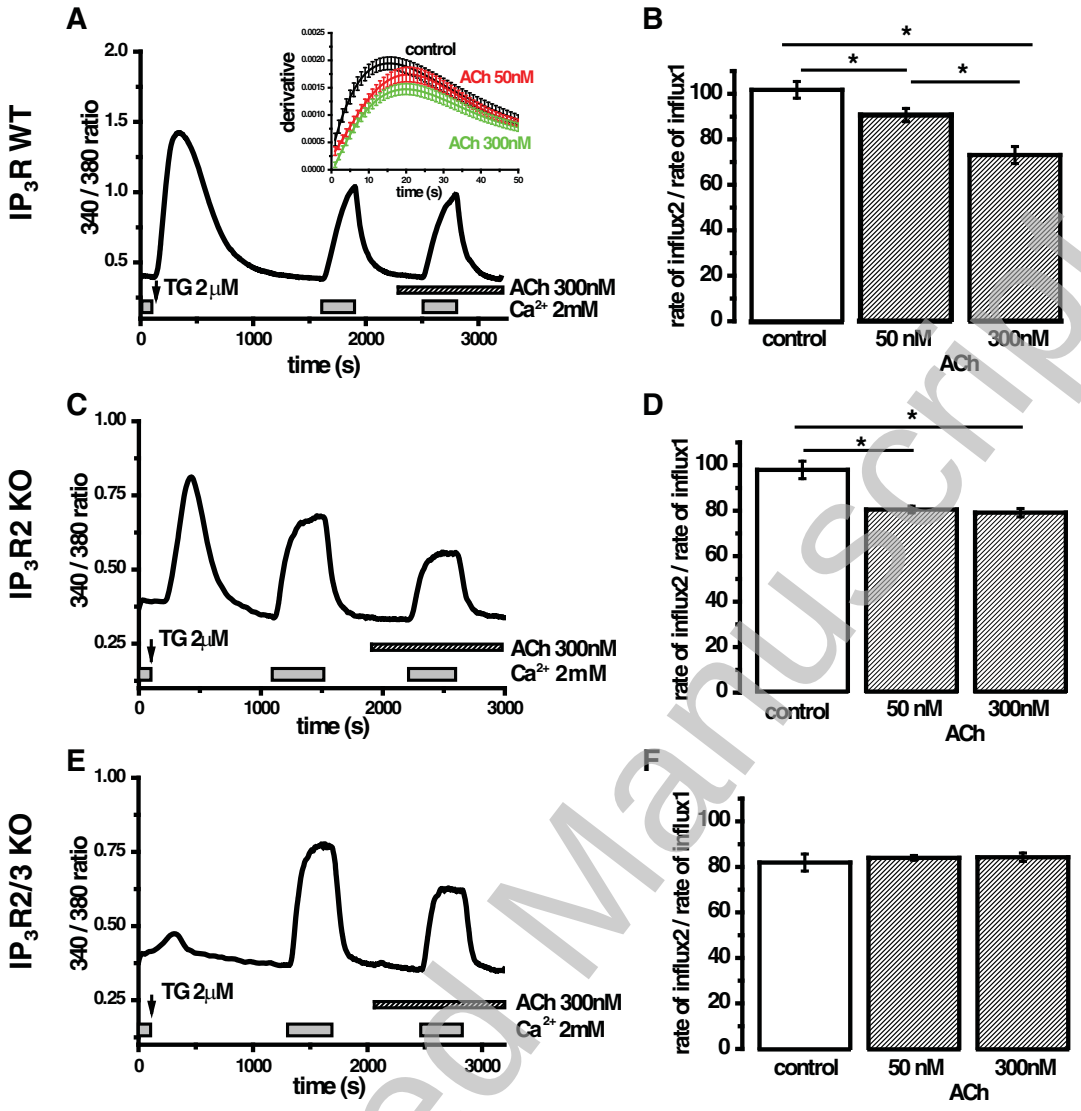

Figure 6